THE JOURNAL OF BIOLOGICAL CHEMISTRY VOL. 284, NO. 15, pp. 10120–10128, April 10, 2009

Expression of the $P2X_7$ Receptor Increases the Ca^{2+} Content of the Endoplasmic Reticulum, Activates NFATc1, and Protects from Apoptosis*

Received for publication, July 29, 2008, and in revised form, December 31, 2008 Published, JBC Papers in Press, February 9, 2009, DOI 10.1074/jbc.M805805200

Elena Adinolfi[1,2], **Maria Giulia Callegari**[1], **Maria Cirillo, Paolo Pinton, Carlotta Giorgi, Dario Cavagna, Rosario Rizzuto**[3], **and Francesco Di Virgilio**

From the Department of Experimental and Diagnostic Medicine, Section of General Pathology, and Interdisciplinary Center for the Study of Inflammation, University of Ferrara, via Borsari 46, 44100 Ferrara, Italy

The $P2X_7$ receptor is known for the cytotoxic activity because of its ability to cause opening of non-selective pores in the plasma membrane and activate apoptotic caspases. A key factor of $P2X_7$-dependent cytotoxicity is the massive intracellular Ca^{2+} increase triggered by its activation. Here we show that $P2X_7$ transfection increased the ability of the endoplasmic reticulum to accumulate, store, and release Ca^{2+}. This caused a larger agonist-stimulated increase in cytosol and mitochondrial Ca^{2+} in $P2X_7$ transfectants than in mock transfected cells. $P2X_7$ transfectants survived and even proliferated in serum-free conditions and were resistant to apoptosis triggered by ceramide, staurosporin, or intracellular Zn^{2+} chelation. Finally, the nuclear factor of activated T cells complex 1 (NFATc1) was strongly activated in the $P2X_7$ transfectants. These observations support our previous finding that the $P2X_7$ receptor under tonic conditions of stimulation, *i.e.* those observed in response to basal ATP release, has an anti-apoptotic or even growth promoting rather than cytotoxic activity.

Cell responses to extracellular ATP are mediated by P2 receptors: ionotropic P2X and metabotropic P2Y (1). The $P2X_7$ receptor ($P2X_7R$)[4] subtype stands out in the P2X subfamily for its ability to trigger a host of physiologic or pathologic responses: plasma membrane blebbing (2, 3), rapid release of interleukin-1β via microvesicle shedding (2, 4), cell fusion (5), lymphoid cell proliferation (6), cell death (7, 8), and bone formation/resorption (9). This receptor is characterized by low affinity for ATP and by two states of permeability (10, 11). At high micromolar ATP concentrations, $P2X_7$ behaves as a cation-selective channel, whereas a prolonged exposure to nearly millimolar concentrations triggers the transition to a nonselective pore that admits hydrophilic solutes of molecular mass up to 900 Da (12–14). A common feature of both conductance states is a strong elevation of free cytoplasmic calcium levels ($[Ca^{2+}]_i$), a response critical for the biological role of this receptor.

Recent evidence from our group shows that basal levels of ATP, naturally present in the extracellular milieu, cause a tonic activation of the $P2X_7R$, which in turn triggers $[Ca^{2+}]_i$ increase and Ca^{2+} entry into the mitochondria. The increased intramitochondrial Ca^{2+} concentration ($[Ca^{2+}]_{mt}$) then enhances mitochondrial potential, increases ATP synthesis, and promotes survival and proliferation in the absence of serum (15). Increased mitochondrial potential and ability to grow under serum-free conditions are hallmark of tumor transformation (16). Furthermore, overexpression of the $P2X_7R$ is associated with several cancers or growth disturbances such as chronic lymphocytic leukemia (17), prostate (18) and breast cancer (19), squamous cell carcinoma (20), nonmelanoma skin cancer (21) neuroblastoma (22), pancreatic tumor (23), thyroid cancer (24), and renal cysts (25).

The endoplasmic reticulum (ER) is the main cellular Ca^{2+} store, characterized by a lumenal Ca^{2+} concentration severalfold higher than the cytoplasm (26). Ca^{+2} is pumped against concentration gradient into the ER by ATPases of the SERCA family, and ER Ca^{2+} concentration ($[Ca^{2+}]_{er}$) is kept constant by spontaneous leak via as yet poorly characterized channels. Thus, SERCA inhibition causes a slow emptying of the ER paralleled by increase in the $[Ca^{2+}]_i$. ER Ca^{2+} can also be transferred to mitochondria at dynamic sites of contact likely controlled by plasma membrane receptors, second messengers, or the metabolic state of the cell (27). ER Ca^{2+} can also be rapidly released upon activation of the IP_3 receptor/channel. The fast $[Ca^{2+}]_i$ transient caused by IP_3 receptor stimulation is a key

* This work was supported, in whole or in part, by National Institutes of Health Grant 1P01AG025532-01A1 (to R. R.). This work was also supported by grants from the Italian Association for Cancer Research (to F. D. V. and P. P.), Telethon of Italy (to F. D. V. and R. R.), the Italian Space Agency (to F. D. V. and R. R.), the Italian Ministry of University and Scientific Research (to F. D. V. and R. R.), the Commission of European Communities 7th Framework Program HEALTH-F2-2007-202231 (to F. D. V.), the PRRIITT program of the Emilia Romagna Region (to R.R and P.P.), the United Mitochondrial Disease Foundation (to P. P.), institutional funds from the University of Ferrara (to F. D. V., R. R., and P. P.), and the project young researchers of the University of Ferrara (to E. A.).

[1] These authors equally contributed to this work.

[2] To whom correspondence should be addressed: Dept. of Experimental and Diagnostic Medicine, Section of General Pathology, Via Borsari 46, 44100 Ferrara, Italy. Tel.: 39-0532-455355; Fax: 39-0532-247278, E-mail: elena.adinolfi@unife.it.

[3] Present address: Dept. of Biomedical Sciences, University of Padova, Italy.

[4] The abbreviations used are: $P2X_7R$, $P2X_7$ receptor; ER, endoplasmic reticulum; SERCA, sarco-endoplasmic reticulum calcium ATPase; IP_3, inositol 1,4,5-trisphosphate; NFATc1, nuclear factor of activated T cells complex 1, HEK293-$P2X_7$, HEK293 cells stably expressing $P2X_7$; HEK293-mock, mock transfected HEK293 cells; oATP, oxidized ATP; tBHQ, *tert*-butylhydroquinone; mtAEQ, mitochondria directed aequorin; erAEQ, ER-directed aequorin; $[Ca^{2+}]_{mt}$, mitochondrial Ca^{2+} concentration $[Ca^{2+}]_{er}$, ER Ca^{2+} concentration; DMEM, Dulbecco's modified Eagle's medium; ELISA, enzyme-linked immunosorbent assay; TPEN, *N*,*N*,*N*′,*N*′-tetrakis(2-pyridylmethyl) ethylenediamine; MOPS, 4-morpholinepropanesulfonic acid.

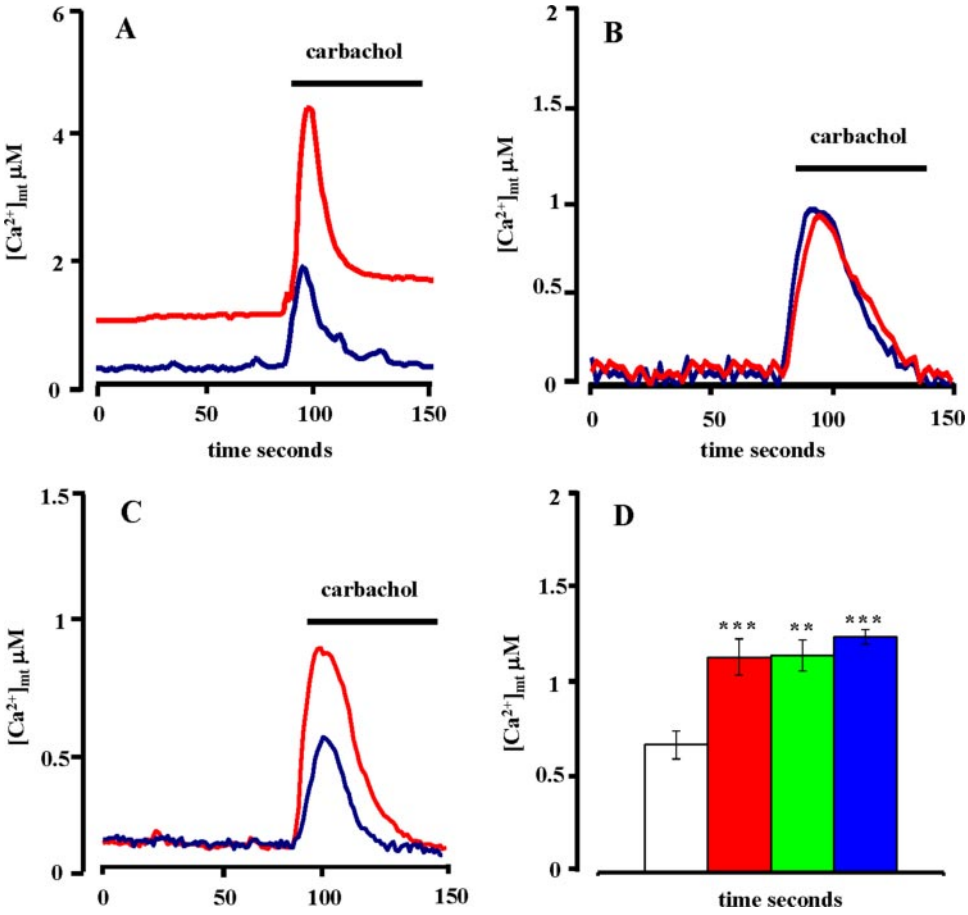

FIGURE 1. **P2X$_7$ expression increases basal and stimulated [Ca^{2+}]$_{mt}$.** Luminescence emission was recorded from HEK293-P2X$_7$ (*red trace*) and HEK293-mock (*blue trace*) cells transfected with mtAEQ as described under "Experimental Procedures" and stimulated with 500 μM carbachol. [Ca^{2+}]$_{mt}$ was determined in the presence of 1 mM extracellular Ca^{2+} (*A* and *B*) or with no Ca^{2+} added and in the presence of 500 μM EGTA (*C* and *D*). In *B* cells were preincubated for 2 h in the presence of 600 μM oATP. Average ± S.E. carbachol-stimulated [Ca^{2+}]$_{mt}$ levels (0.820 + 0.006 and 0.930 + 0.04 μM for mock-and P2X$_7$-transfected cells, respectively) were not statistically different. *D*, summary data of several independent measurements ($n = 6$) of carbachol-stimulated [Ca^{2+}]$_{mt}$ increases in Ca^{2+}-free-EGTA-supplemented medium from mock transfected cells (*empty bar*) and three different HEK293-P2X$_7$ clones. **, $p < 0.01$; ***, $p < 0.001$.

signal for cell proliferation (28). The $[Ca^{2+}]_i$ rise activates multiple enzyme pathways, including calcineurin. Calcineurin in turn causes dephosphorylation of nuclear factor of activated T cells (NFAT) family members that translocate to the nucleus to activate gene transcription (29). Inhibition of calcineurin phosphatase activity by FK506, cyclosporin A, or new drugs such as VIVIT blocks NFAT translocation to the nucleus and DNA binding (30). The calcineurin pathway is so important for T cell proliferation that FK506 and cyclosporin are widely used as immunosuppressants (31, 32). In addition to immune cells, members of the NFAT family are also expressed in a wide range of other cell types where they are implicated in cell cycle progression, cell development and differentiation, angiogenesis, and tumorigenesis (33, 34). The NFAT family comprises four members, among which NFATc1 plays a key role in cell growth as shown by the phenotype of the NFATc1 KO mice, which exhibits serious B and T lymphocyte, cardiomyocyte, and osteoblast deficit (35). Moreover, NFATc1 is activated in pancreatic cancer overexpressing the c-*myc* oncogene (34) and is implicated in resistance to apoptosis (36) and in tumor invasiveness (37).

In a previous study we showed that HEK293 cells transfected with the P2X$_7$R (HEK293-P2X$_7$) have a higher resting mitochondrial Ca^{2+} ([Ca^{2+}]$_{mt}$) and release a larger amount of Ca^{2+} from intracellular stores following stimulation of plasma membrane receptors coupled to IP$_3$ generation (15). In the present study we show that P2X$_7$ expression increases ER Ca^{2+} uptake and steady-state level, activates NFATc1, enhances cell survival, and protects from apoptosis.

EXPERIMENTAL PROCEDURES

Reagents and Antibodies—ATP was purchased from Roche Applied Science. Oxidized ATP (oATP), benzoylbenzoic ATP, carbachol, ceramide, staurosporin, *tert*-butylhydroquinone (tBHQ), thapsigargin, and TPEN were purchased from Sigma-Aldrich. fura 2/acetoxymethylester and coelenterazine were from Invitrogen-Molecular Probes (San Giuliano Milanese, Italy). VIVIT and rabbit polyclonal anti-P2X$_7$ antibodies were purchased from Calbiochem (Merck KGaA associate company, Darmstadt, Germany). The anti-SERCA2 mouse monoclonal antibody and horseradish peroxidase-conjugated goat anti mouse, were from AbCam (Cambridge, UK). Peroxidase-linked protein A was from Amersham Biosciences.

Cell Culture and Transfection—HEK293 and NIH3T3 cells were cultured in DMEM-F12 (Sigma-Aldrich) or DMEM (Sigma-Aldrich) medium, respectively, supplemented with 10% fetal calf serum (Invitrogen), penicillin (100 units/ml) (Euro Clone, Pero, Milano, Italy), and streptomycin (100 mg/ml) (Euro Clone). Stable clones transfected with the human P2X$_7$R were kept in the continuous presence of 0.2 mg/ml G418 sulfate (Geneticin, Calbiochem). The experiments, unless otherwise indicated, were performed in the following saline solution, also referred to as "standard saline" in the text: 125 mM NaCl, 5 mM KCl, 1 mM $MgSO_4$, 1 mM NaH_2PO_4, 20 mM HEPES, 5.5 mM glucose, 5 mM $NaHCO_3$, pH 7,4. When indicated, 1 mM $CaCl_2$ or 500 μM EGTA was added. The cells were transfected with the calcium phosphate method as described previously (15). To exclude possible effects of clonal selection, all of the experiments were performed with three different stable HEK293 clones expressing the P2X$_7$R (15). Although not shown in the figures, all conditions tested for mock transfected HEK293 cells (HEK293-mock) were also assayed for wild type HEK293 cells. NIH3T3 fibroblasts were transiently transfected with Lipofectamine 2000 (Invitrogen) as described by the manufacturer.

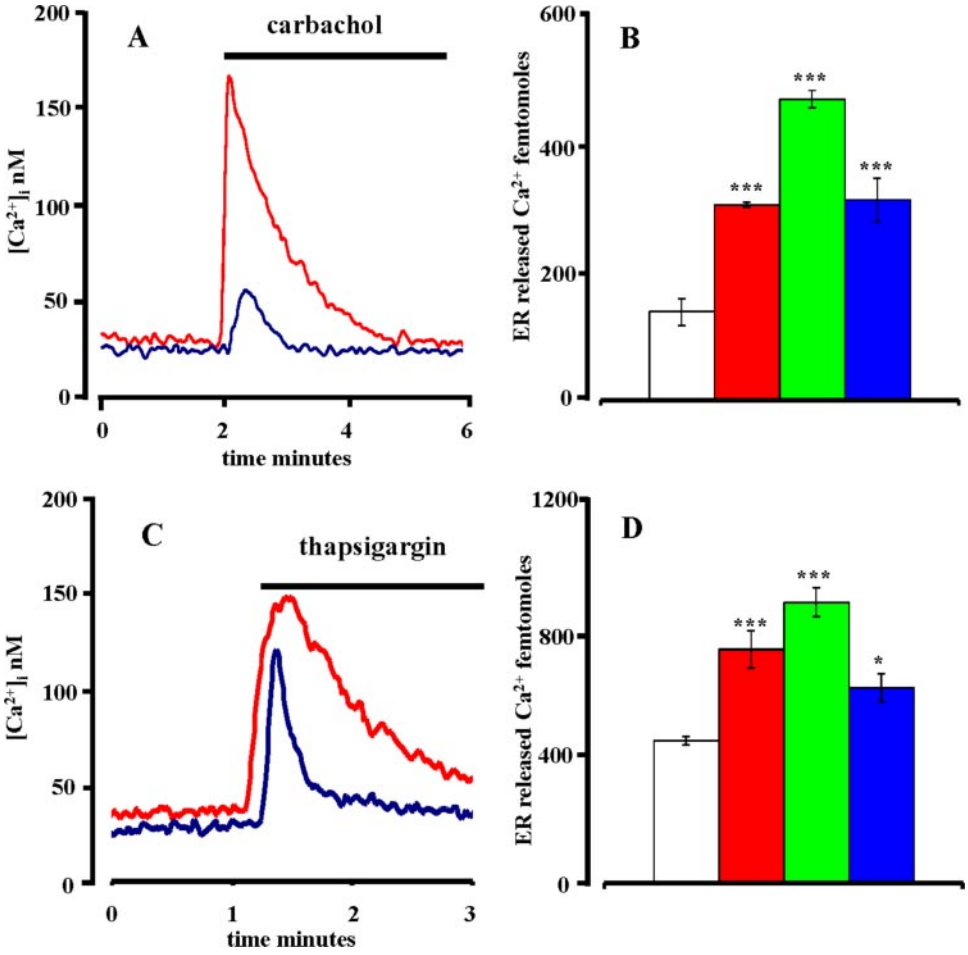

FIGURE 2. **P2X$_7$ expression enhances agonist-stimulated mobilization of intracellular [Ca^{2+}]$_i$.** fura-2-loaded HEK293-P2X$_7$ (*red trace*) and HEK293-mock (*blue trace*) cells were incubated in a fluorimeter cuvette at a concentration of 10^6/ml. Carbachol (*A* and *B*) or thapsigargin (*C* and *D*) were added at the concentration of 500 and 2 μM, respectively. *B* and *D*, summary data of repeated ($n = 6$) [Ca^{2+}]$_i$ determinations from mock transfected cells (*empty bar*) and three different HEK293-P2X$_7$ clones. The absolute amount of Ca^{2+} released by carbachol and thapsigargin was determined by measuring the area under the peak as described under "Experimental Procedures." *, $p < 0.05$; ***, $p < 0.001$.

Briefly plasmid and transfection reagent were resuspended in Opti-MEM medium (Invitrogen) at a ratio of 2 μl of Lipofectamine/1 μg of DNA, mixed and administered to cells at a final concentration of 1 μg of DNA/10^5 cells. The experiments were performed 48 h after transfection. For [Ca^{2+}]$_{mt}$ measurements, double transfection was obtained at a 3:1 P2X$_7$R/mtAEQ plasmid ratio. Aequorins selectively targeted to the endoplasmic reticulum (erAEQ) or the mitochondria (mtAEQ) were previously engineered in Professor Rizzuto's laboratory (38).

Measurement of [Ca^{2+}]$_i$—[Ca^{2+}]$_i$ measurements were performed in a thermostat-controlled and magnetically stirred PerkinElmer Life Sciences fluorimeter with the fluorescent indicator fura 2/acetoxymethylester. Briefly the cells were loaded with 4 μM fura 2/acetoxymethylester for 20 min in 1 mM Ca^{2+}-supplemented standard saline in the presence of 250 μM sulfinpyrazone in standard saline, rinsed, and resuspended in the appropriate saline solution at a final concentration of 10^6/ml. Excitation and emission wavelengths were 340/380 and 505 nm, respectively.

Measurement of [Ca^{2+}]$_{er}$ and [Ca^{2+}]$_{mt}$—[Ca^{2+}]$_{er}$ was measured according to the protocol described previously (38). Cells were plated at a density of 5×10^4 onto 13 mm coverslips and transfected with the erAEQ plasmid. To allow accurate [Ca^{2+}]$_{er}$ measurement, erAEQ must be reconstituted with coelenterazine in the absence of Ca^{2+}. To this aim, the cells were incubated at 20 °C for 10 min in AEQ buffer: 135 mM NaCl, 5 mM KCl, 0.4 mM KH_2PO_4, 1 mM $MgSO_4$, 5,5 mM glucose, and 20 mM HEPES, pH 7.4, in the presence of 600 μM EGTA and 50 μM tBHQ, a reversible inhibitor of SERCA pumps, to deplete ER Ca^{2+} (38). At the end of this incubation, erAEQ was reconstituted with its cofactor coelenterazine (5 μM) for 45 min at room temperature. The coverslips were mounted in a perfused and thermostated chamber hosted in a custom-made, high sensitivity luminometer. To remove tBHQ prior to Ca^{2+} measurements, the cells were perfused for 2 min with AEQ buffer supplemented with 100 μM EGTA. Perfusion was then switched to 1 mM $CaCl_2$-containing AEQ buffer to measure kinetics of ER Ca^{2+} uptake and the ensuing steady-state level. The experiment was terminated by lysing the cells with 100 μM digitonin in a hypotonic Ca^{2+}-rich solution (10 mM $CaCl_2$ in H_2O) to discharge the residual ER AEQ pool and allow calibration of the AEQ signal.

[Ca^{2+}]$_{mt}$ was measured with mtAEQ. Cells were plated at a density of 5×10^4 onto 13-mm coverslips and transfected with the mtAEQ plasmid or, in the case of NIH3T3 cells, with mtAEQ plus P2X$_7$R. mtAEQ was reconstituted for 2 h at 37 °C in AEQ buffer supplemented with 1 mM $CaCl_2$ and 5 μM coelenterazine. Perfusion was performed with AEQ buffer plus 500 μM EGTA or, alternatively, 1 mM $CaCl_2$. After stabilization of the light signal, 500 μM carbachol was added to the perfusion solution.

The light signal from mtAEQ- or erAEQ-transfected cells was collected with a low noise photomultiplier with built-in amplifier discriminator. The output of the discriminator was captured by a Thorn-EMI photon counting board and stored in an IBM-compatible computer for further analyses. The AEQ luminescence data were calibrated off-line into [Ca^{2+}] values using a computer algorithm based on the Ca^{2+} response curve of wild type and mutant AEQs, as described previously (39, 40). Rate of ER calcium uptake was calculated as first derivative of kinetics of ER Ca^{2+} uptake (see Fig. 3*A*). The total amount of released Ca^{2+} was measured as second derivative of [Ca^{2+}]$_i$ increase measured with fura-2. Origin software was used for

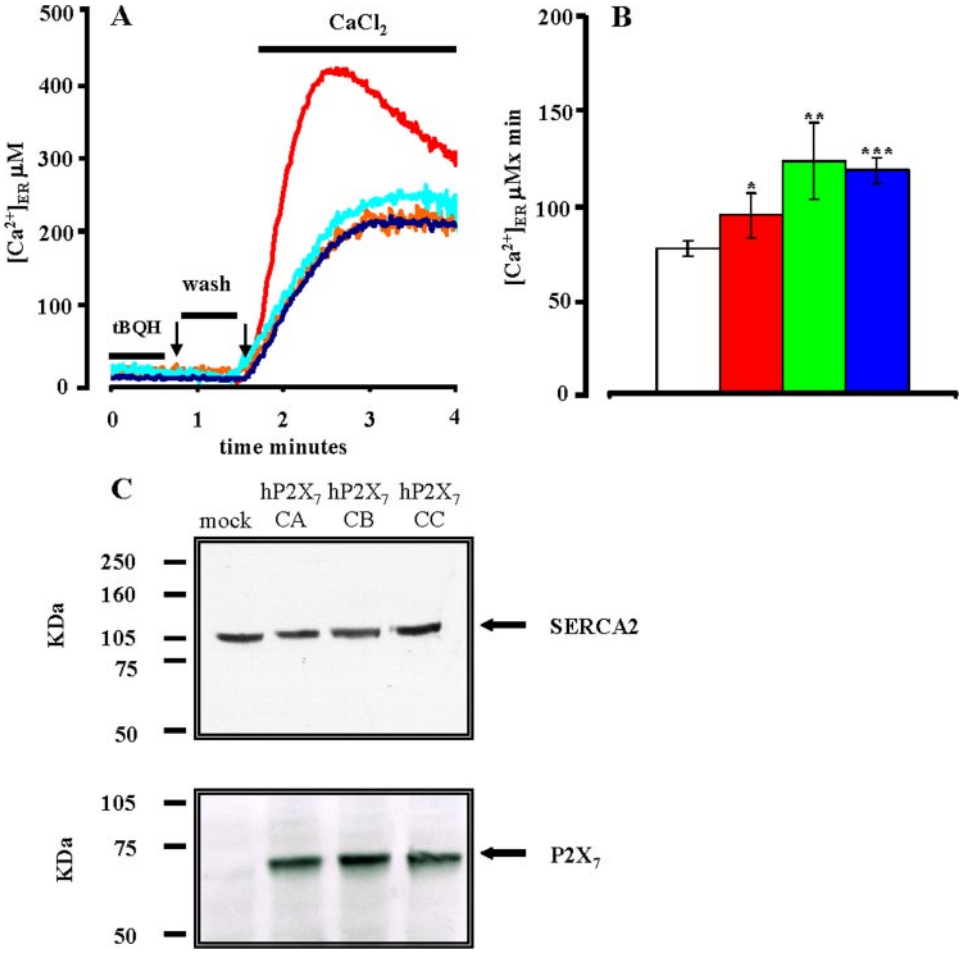

FIGURE 3. **Rate of ER calcium uptake is enhanced in HEK293-P2X$_7$ cells.** *A*, HEK293-P2X$_7$ and HEK293-mock cells were pretreated with 50 μM tBHQ in AEQ buffer supplemented with 600 μM EGTA and 5 μM coelenterazine to discharge ER Ca^{2+} and reconstitute erAEQ. At the end of this incubation, they were placed into the luminometer chamber, rinsed to remove tBHQ, and perfused with 1 mM Ca^{2+}-containing AEQ buffer. This procedure allows calculation of initial rate of ER Ca^{2+} uptake. Where required, prior to tBHQ incubation, the cells were treated with 600 μM oATP for 2 h. HEK293-P2X$_7$ (*red trace*), HEK293-mock (*blue trace*), HEK293-P2X$_7$ pretreated with oATP (*orange trace*), and HEK293-mock pretreated with oATP (*cyan trace*). *B*, summary of ER uptake rate (measured as μM increase/min) in HEK293-mock and in three different HEK293-P2X$_7$ cell clones ($n = 6$). *, $p \leq 0.05$; **, $p \leq 0.01$. *C*, SERCA2 and P2X$_7$ expression in mock transfected and stably transfected HEKhP2X$_7$ cell clones. *Lane 1*, HEK293-mock cells; *lane 2*, HEK293-P2X$_7$ clone A; *lane 3*, HEK293-P2X$_7$ clone B; *lane 4*, HEK293-P2X$_7$ clone C.

both calculations (OriginLab, Northampton, MA). A mean cell radius of 10 μm was measured by confocal microscopy giving an approximate cell volume of 4.2 picoliters.

Cell Proliferation and Viability Assay—Cell proliferation of HEK293 cells was measured by direct count. To this purpose, 10^5/ml cells were seeded in six-well Falcon plates (BD Biosciences, Lincoln Park, NJ) in serum-free DMEM-F12 medium in the presence or absence of various stimuli and placed in a CO_2 incubator at 37 °C. At the appropriate time cells were detached and counted in a Burker chamber with an Olympus IMT-2 (Olympus Corporation, Tokio, Japan) microscope equipped with a 40× phase contrast objective. Proliferation of NIH3T3 cells was assayed with the 3-(4,5-dimethylthiazol-2-yl)-2,5-diphenyltetrazolium bromide test 48 h after transfection with P2X$_7$-containing or empty plasmid. Briefly, 5×10^4 cells were incubated for 3 h in 1 mM Ca^{2+}-supplemented standard saline in the presence of 0.5 mg/ml of dimethyltiazol diphenyltetrazolium bromide (Sigma-Aldrich), rinsed, and further incubated for 15 min in 90% isopropanol plus 10% DMSO. Absorbance was measured at 540 nm in a VICTOR^3 spectrophotometer (PerkinElmer Life Sciences). Cell viability was also assessed with the trypan blue assay. The cells were washed and incubated in phosphate-buffered saline, 0.4% trypan blue stain solution for 5 min at room temperature and then counted. Apoptosis was evaluated with the cell death ELISA plus kit (Roche Applied Science). 10^4 cells/sample were plated in 48-well plates (Falcon) and challenged with the different stimuli. The cells were then lysed, and histone-associated DNA fragments were measured.

Morphological Analysis—The images were acquired with a Nikon Eclipse TE300 inverted microscope (Nikon, Tokyo, Japan) equipped with a thermostatted chamber (Bioptechs, Butler, PA) and a 63× oil immersion objective.

Western Blot—The cells were lysed by repeated freeze-thawing cycles in standard saline solution supplemented with protease inhibitors. The cell lysates (15 μg of total protein) were loaded on a Bis-Tris 4–12% NuPage acrylamide gel (Invitrogen) with MOPS buffer (Invitrogen), and electrophoretically transferred to Hybond-ECL nitrocellulose membranes (Amersham Biosciences). Primary antibodies were used at a 1:2000 (SERCA) and 1:300 (P2X$_7$) dilutions. Secondary reagents, goat anti-mouse (AbCam) or protein A (Amersham Biosciences), were added to the blocking solution at a 1:3000 dilution.

Measurement of NFATc1 Activation—Nuclear extracts were obtained with the nuclear extract kit (Active Motif, Rixensart, Belgium). NFATc1 was measured with the TransAM NFATc1 ELISA kit (Active Motif) as described by the manufacturer.

Data Analysis—All of the data are shown as the averages ± S.E. of the mean. Tests of significance were performed by Student-Newman-Keul's test using Graphpad InStat software (Graphpad, San Diego, CA).

RESULTS

HEK293-P2X$_7$ Cells Have an Increased Intracellular Store Ca^{2+} Content—As previously reported (15), $[Ca^{2+}]_{mt}$ level was 3–4-fold higher in HEK293-P2X$_7$ than in mock transfected cells. Accordingly, the $[Ca^{2+}]_{mt}$ transient in response to an agonist coupled to IP_3 generation (carbachol) was at least twice as high. Oxidized ATP is a powerful blocker of the P2X$_7$R (41).

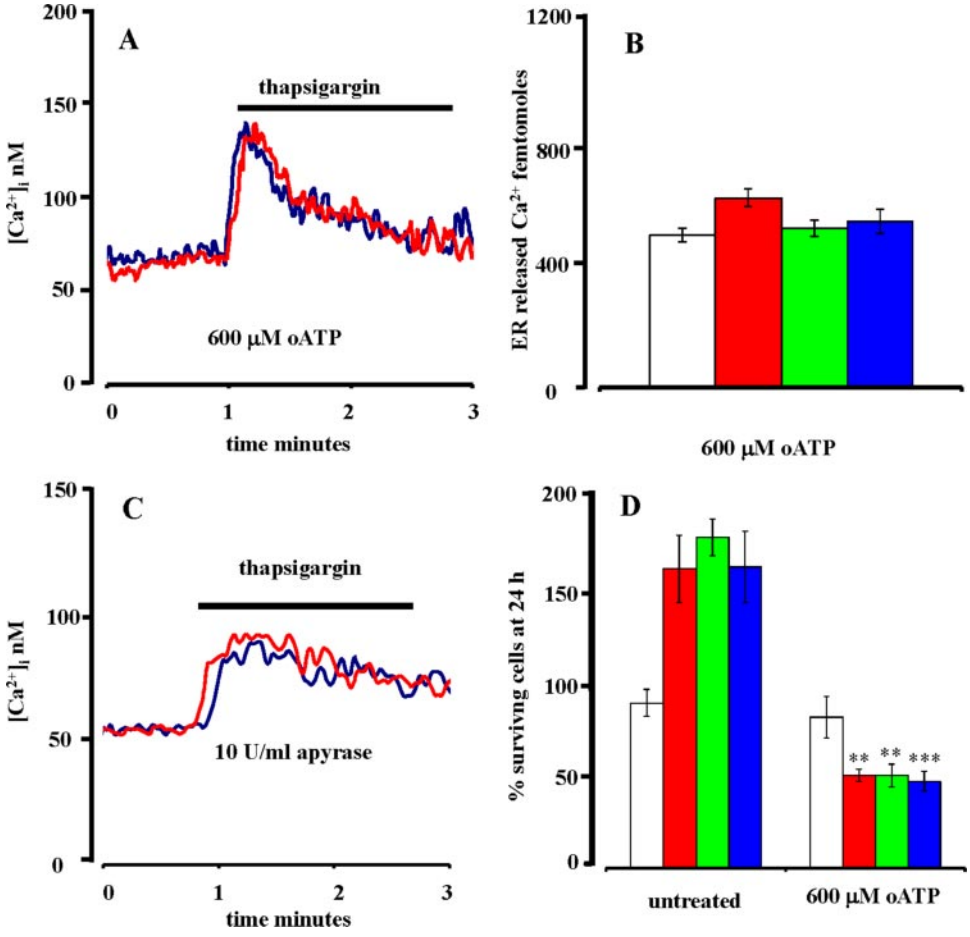

FIGURE 4. **Increased $[Ca^{2+}]_{er}$ depends on P2X$_7$ function and correlates with cell survival.** *A*, fura-2-loaded HEK293-P2X$_7$ (*red trace*) and HEK293-mock (*blue trace*) cells were pretreated with 600 μM oATP, incubated in a fluorimeter cuvette in standard saline solution supplemented with 500 μM EGTA at a 10^6/ml concentration and challenged with 2 μM thapsigargin. *B*, summary data of thapsigargin-releasable Ca^{2+} determined as described in Fig. 2, from HEK293-mock cells (*white bar*), or three different HEK293-P2X$_7$ clones in the absence or presence oATP ($n = 3$). *C*, effect of preincubation with apyrase (10 units/ml for 30 min) on thapsigargin-releasable Ca^{2+}. The cells were incubated in 500 μM EGTA-containing standard saline and stimulated with 2 μM thapsigargin. The release rate of ER Ca^{2+} in the presence of apyrase was not statistically different in HEK293-P2X$_7$ and HEK293-mock cells. *D*, summary data of 24 h survival under serum-free conditions of HEK293-mock cells (white) or different HEK293-P2X$_7$ clones in the absence or presence oATP are shown ($n = 15$). **, $p \leq 0.01$; ***, $p \leq 0.001$.

Despite its low selectivity, this inhibitor is a useful tool for the investigation of P2X$_7$R function because it covalently modifies the receptor, thus causing an irreversible inactivation. Furthermore, countless *in vitro* and *in vivo* experiments have shown that long lasting exposure to this inhibitor has no untoward effects on cell viability (42, 43). Differences in $[Ca^{2+}]_{mt}$ levels depended on a functional P2X$_7$ receptor as preincubation in the presence of oATP (2 h) equalized basal as well as carbachol-stimulated $[Ca^{2+}]_{mt}$ of P2X$_7$- and mock-transfected HEK293 cells (Fig. 1*B*). Basal $[Ca^{2+}]_{mt}$ was closely dependent on Ca^{2+} influx because it was obliterated by chelation of extracellular Ca^{2+} (Fig. 1*C*). The carbachol-stimulated $[Ca^{2+}]_{mt}$ rise was also affected by removal of extracellular Ca^{2+} but to a lesser extent than by preincubation in the presence of oATP. This is likely due to the brief (10 min) incubation under Ca^{2+}-free conditions. To exclude clonal selection artifacts, carbachol-stimulated $[Ca^{2+}]_{mt}$ levels were measured in three different HEK293-P2X$_7$ stable clones (Fig. 1*D*). These clones were used throughout this study. As an average, carbachol-stimulated $[Ca^{2+}]_{mt}$ of HEK293-P2X$_7$ cells was at least twice as high as in mock transfected cells. Release of Ca^{2+} into the cytosol in response to carbachol or thapsigargin was also much higher in the P2X$_7$-transfectants than in mock transfected cells (Fig. 2). These experiments suggested that transfection with the P2X$_7$R conferred a stronger ability to accumulate Ca^{2+} into the ER. In support of this suggestion we observed that rate of Ca^{2+} uptake into the ER was significantly higher in HEK293-P2X$_7$ than in mock transfected or wild type HEK293 cells (Fig. 3, *A* and *B*). This difference was completely obliterated by pretreatment with the P2X$_7$ covalent inhibitor oATP (Fig. 3*A*). The increased Ca^{2+} uptake is likely to depend on a higher efficiency of the SERCA pumps because the level of SERCA protein expression did not differ between P2X$_7$- and mock transfected cells (Fig. 3*C*).

Blockade of P2X$_7$R Normalizes $[Ca^{2+}]_{er}$ and Obliterates the Growth Advantage of HEK293-P2X$_7$ Cells—We then investigated the dependence of $[Ca^{2+}]_{er}$ on a functional P2X$_7$ receptor. Fig. 4 (*A* and *B*) shows that treatment of HEK293-P2X$_7$ and mock transfected cells with oATP prior to stimulation with thapsigargin fully obliterated the difference in ER Ca^{2+} content between the two cell populations. It is likely that tonic activation of P2X$_7$ was responsible for supporting a larger Ca^{2+} influx from the extracellular space and therefore also a larger ER accumulation. Because HEK293 cells constantly release ATP into the pericellular space, we tested the effect of the ATP-hydrolyzing enzyme apyrase. As shown in Fig. 4*C*, preincubation in the presence of apyrase obliterated the differences in ER Ca^{2+} content between P2X$_7$-transfected and mock transfected cells. In addition, oATP treatment abrogated the growth advantage of HEK293-P2X$_7$ (Fig. 4*D*). Notice that oATP treatment had no effect on ER Ca^{2+} content or survival of mock transfected cells.

P2X$_7$ Transfectants Are Resistant to Various Apoptotic Stimuli—We next investigated whether HEK293-P2X$_7$R cell clones were also more resistant to cell death induced by different stimuli in addition to serum deprivation. Three agents were investigated: C2 ceramide, staurosporin, and the membrane-permeant Zn^{2+}-chelating agent TPEN. As shown in Fig. 5, in the presence of extracellular Ca^{2+}, challenge with C2 ceramide caused shrinkage and plasma membrane blebbing in mock transfected cells. On the contrary, no such changes were

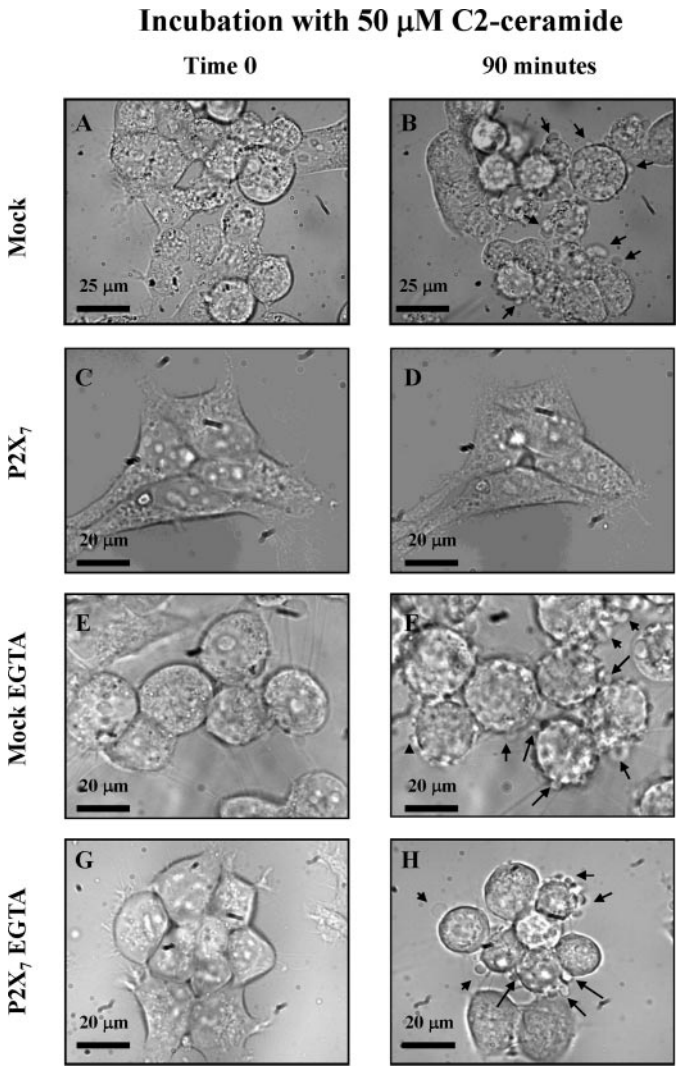

FIGURE 5. **Delayed blebbing in C2-ceramide-treated HEK293-P2X$_7$ cells.** HEK293-P2X$_7$ and HEK293-mock cells were plated on coverslips at a concentration of 10^5/ml in standard saline supplemented with 1 mM Ca^{2+} or with 500 μM EGTA. The coverslips were transferred to the thermostated stage of an inverted Nikon Eclipse 300 microscope, and 50 μM C2 ceramide was added. The images were acquired every 15 min for a total of 90 min. *A*, *B*, *E*, and *F*, HEK293-mock cells; *C*, *D*, *G*, and *H*, HEK293-P2X$_7$. *A–D*, standard saline solution plus 1 mM Ca^{2+}. *E–H*, standard saline solution plus 500 μM EGTA.

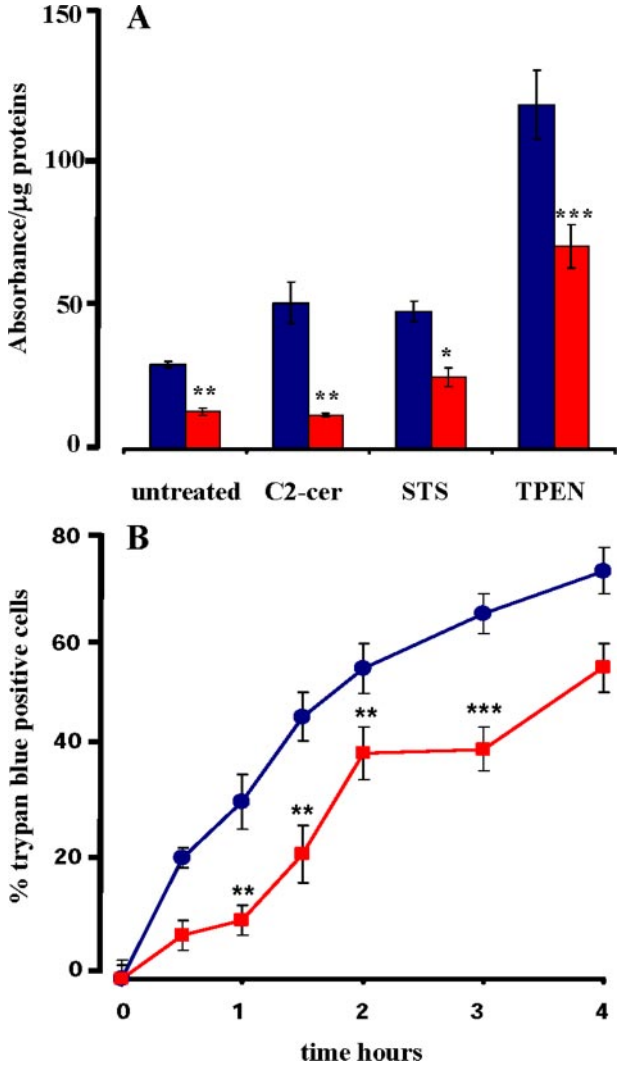

FIGURE 6. **HEK293-P2X$_7$ cells are protected from apoptosis.** *A*, HEK293-P2X$_7$ (*red*) and HEK293-mock cells (*blue*) were suspended in serum-free DMEM medium, plated in 48 well dishes at a concentration of 5×10^4/ml, and challenged with C2 ceramide (20 μM), staurosporin (STS, 10 μM), or TPEN (4 μM). Apoptosis was evaluated as described under "Experimental Procedures" after 2 h (ceramide) or 16 h (staurosporin and TPEN). *B*, kinetics of C2-ceramide-stimulated trypan blue uptake from HEK293-P2X$_7$ (*red*) and HEK293-mock cells (*blue*). The cells were suspended in standard saline, plated in 48-well dishes at a concentration of 5×10^4, and challenged with C2-ceramide (20 μM). Basal trypan blue uptake at time 0 (about 15% of total) was subtracted from all values. **, $p < 0.01$; ***, $p < 0.001$ ($n = 9$).

induced in HEK293-P2X$_7$ cells. The protective effect of P2X$_7$ expression was abrogated by removal of extracellular Ca^{2+}, suggesting that the elevated $[Ca^{2+}]_{mt}$ levels in resting conditions play a critical role in the inhibition of the apoptotic process. The morphological alterations typical of apoptosis were corroborated by ELISA analysis of DNA fragmentation (Fig. 6*A*).

HEK293-P2X$_7$ cells were refractory to apoptosis induced by any of the three pro-apoptotic agents used. Apoptotic cells in culture undergo a terminal increase in plasma membrane permeability, which can be monitored by the usual trypan blue uptake test. Even this gross index of cell death confirmed the lower susceptibility of HEK293-P2X$_7$ to cytotoxic stimulation (Fig. 6*B*).

Enhanced Survival of HEK293-P2X$_7$ Cells Depends on NFATc1 Activation—Calmodulin/calcineurin/NFAT is the main intracellular survival/growth-promoting pathway activated by mobilization of ER Ca^{2+} and the associated $[Ca^{2+}]_i$ increases (34). Thus, we hypothesized that the survival/growth advantage of HEK293-P2X$_7$ cells might depend on NFAT activation. As shown in Fig. 7*A* this anticipation was fulfilled, because HEK293-P2X$_7$ cells displayed a level of NFATc1 activation about twice as high as mock transfected cells. To support the key role played by P2X$_7$ and extracellular ATP in this process, enhanced NFATc1 activation was reverted by treatment with oATP or apyrase. In addition, the selective membrane-permeant blocker VIVIT, a peptide that blocks interaction between calcineurin and NFATc1, abrogated the higher NFATc1 activation level of HEK293-P2X$_7$. Accordingly, incubation in the presence of VIVIT or cyclosporin also abrogated the survival/growth advantage of the P2X$_7$ transfectants.

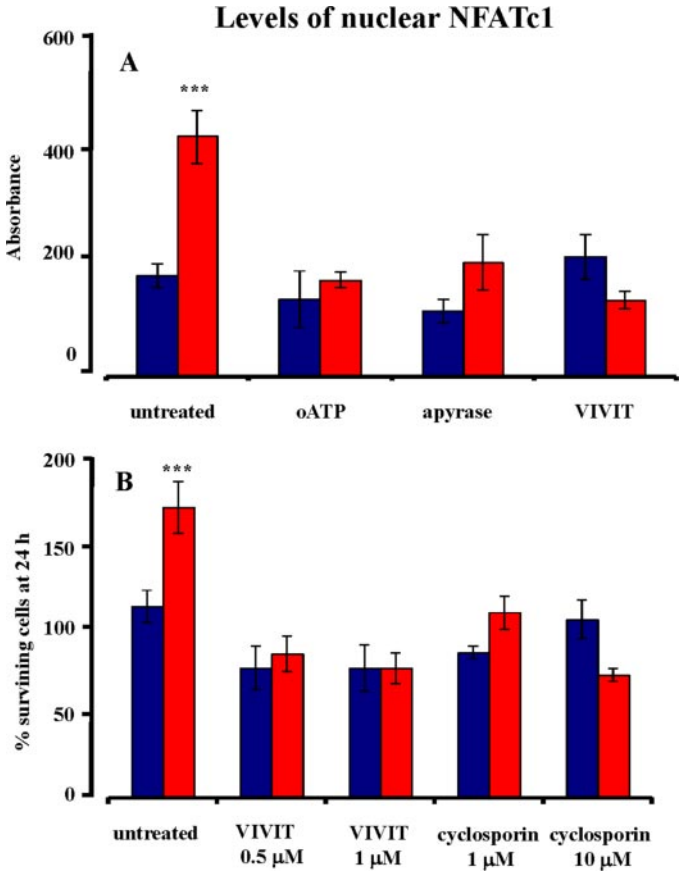

FIGURE 7. **Increased NFATc1 activation in HEK293-P2X$_7$ cells.** *A*, HEK293-mock and HEK293-P2X$_7$ (clone A) were incubated for 16 h in serum free DMEM-F12 medium at 37 °C supplemented with either oATP (600 μM), apyrase (1 unit/ml), or VIVIT (1 μM). After this incubation time, the cells were rinsed and detached, and nuclear extracts were obtained as described under "Experimental Procedures." Nuclear translocation of NFATc1 was measured by ELISA. *B*, mock transfected (*blue*) or HEK293-P2X$_7$ (*red*) cells were incubated at 37 °C in serum free DMEM-F12 medium in the absence or presence of VIVIT or cyclosporin for 24 h. At the end of this incubation, the cells were rinsed, detached, and counted. Similar data were obtained with two other stable HEK293-P2X$_7$ clones. ***, $p < 0.001$ ($n = 6$).

P2X$_7$ Transfection Increases NFATc1 Activation, Enhances Growth, and Increases [Ca^{2+}]$_{mt}$ in NIH3T3 Cells—To show that the trophic effect of P2X$_7$ transfection is not restricted to a single cell line (HEK293 cells) but is likely to be widespread, we also run key experiments in another widely used cell line, NIH3T3 cells. As shown in Fig. 8, even in this mouse cell line P2X$_7$ transfection enhanced NFATc1 nuclear levels (Fig. 8*A*), proliferation (Fig. 8*B*), and $[Ca^{2+}]_{mt}$ in response to a Ca^{2+}-mobilizing agonist (Fig. 8, *C* and *D*). To increase $[Ca^{2+}]_{mt}$, bradykinin was used instead of carbachol because NIH3T3 cells did not respond to this latter agonist. At variance with HEK293-P2X$_7$, P2X$_7$ transfection did not increase basal $[Ca^{2+}]_{mt}$, a difference likely caused by the fact that NIH3T3 cells were transiently transfected, while HEK293 cells were stably transfected.

DISCUSSION

P2X$_7$R is the prototypic cytotoxic P2 receptor. However, increasing evidence, mainly from our laboratory, suggests that the P2X$_7$R may also have an apparently paradoxical survival/growth promoting effect. Long ago we made the observation that heterologous expression of this receptor confers a growth advantage in the absence of serum (6). Furthermore, several tumors express high level of P2X$_7$R protein (15). This finding is under evaluation for the design of novel anticancer therapies based on the administration of potent P2X$_7$R agonists that may cause a selective deletion of tumor cells. However, given the widespread presence of ATP in tissue interstitium, we believe it unlikely that tumor cells overexpress a potentially lethal receptor unless this turns out of advantage for the tumor cells. Thus, the growth promoting activity of P2X$_7$R was of no surprise to us. The intracellular pathways involved in this effect are as yet largely unknown; however data shown in this and our previous work point to at least four major players: Ca^{2+}, mitochondria, ER, and NFATc1.

The ability of HEK293-P2X$_7$ to accumulate an increased amount of Ca^{2+} from extracellular medium is a necessary feature of the growth advantage as removal of extracellular Ca^{2+} abolishes this advantage (15). $[Ca^{2+}]_{mt}$ seems to be more important than $[Ca^{2+}]_i$ because we were unable to find consistently elevated $[Ca^{2+}]_i$ levels in resting conditions in HEK293-P2X$_7$, while on the contrary a higher $[Ca^{2+}]_{mt}$ is a constant finding. In the present study we show that in addition to $[Ca^{2+}]_{mt}$, $[Ca^{2+}]_{er}$ is also higher in HEK293-P2X$_7$ than in mock transfected cells. Thus, it is likely that the higher $[Ca^{2+}]_{mt}$ depends on the higher $[Ca^{2+}]_{er}$ level. Given the presence of contacts between mitochondria and the ER, it is possible that ER Ca^{2+} is directly transferred to the mitochondrial matrix or alternatively is first discharged into the cytoplasm and subsequently taken up by the mitochondria.

The increased ER Ca^{2+} content is due to enhanced ER accumulating ability. We initially hypothesized that this might be due to a higher expression level of SERCAs, but this is not the case because the level of expression of these enzymes is unchanged in wild type, mock transfected, or P2X$_7$-transfected cells. Alternatively, functional activity of SERCAs might be increased in HEK293-P2X$_7$ cells, but clarification of this issue requires further investigation.

The ability to withstand unfavorable environmental conditions seems to be a distinct feature of HEK293-P2X$_7$ because additional apoptotic stimuli, together with serum starvation, are less effective in these than in mock transfected cells. The cellular mechanism is likely to involve multiple cellular pathways, including Ca^{2+}-dependent processes. The protective role of $[Ca^{2+}]_{er}$ is clearly shown by experiments performed in cells chronically exposed to EGTA, a condition that brings the level of $[Ca^{2+}]_{er}$ of HEK293-P2X$_7$ cells to the same level of HEK293-mock.

The relationship between $[Ca^{2+}]_{er}$ and cell death is rather complex. There is a substantial body of data showing that reducing $[Ca^{2+}]_{er}$ has a protective effect against apoptosis dependent on stimuli releasing Ca^{2+} from intracellular stores (44–46). Accordingly, procedures that lower the ER Ca^{2+} content or prevent transfer of ER Ca^{2+} to the mitochondria also prevent apoptosis (47). In principle, P2X$_7$R-expressing cells should be "primed" for apoptosis because resting $[Ca^{2+}]_{er}$ and $[Ca^{2+}]_{mt}$ are elevated, but this is not the case. Because enhanced transfer of ER Ca^{2+} to the mitochondria has been identified as key step by which an increased $[Ca^{2+}]_{er}$ may accelerate apoptosis, it might be hypothesized that P2X$_7$R expres-

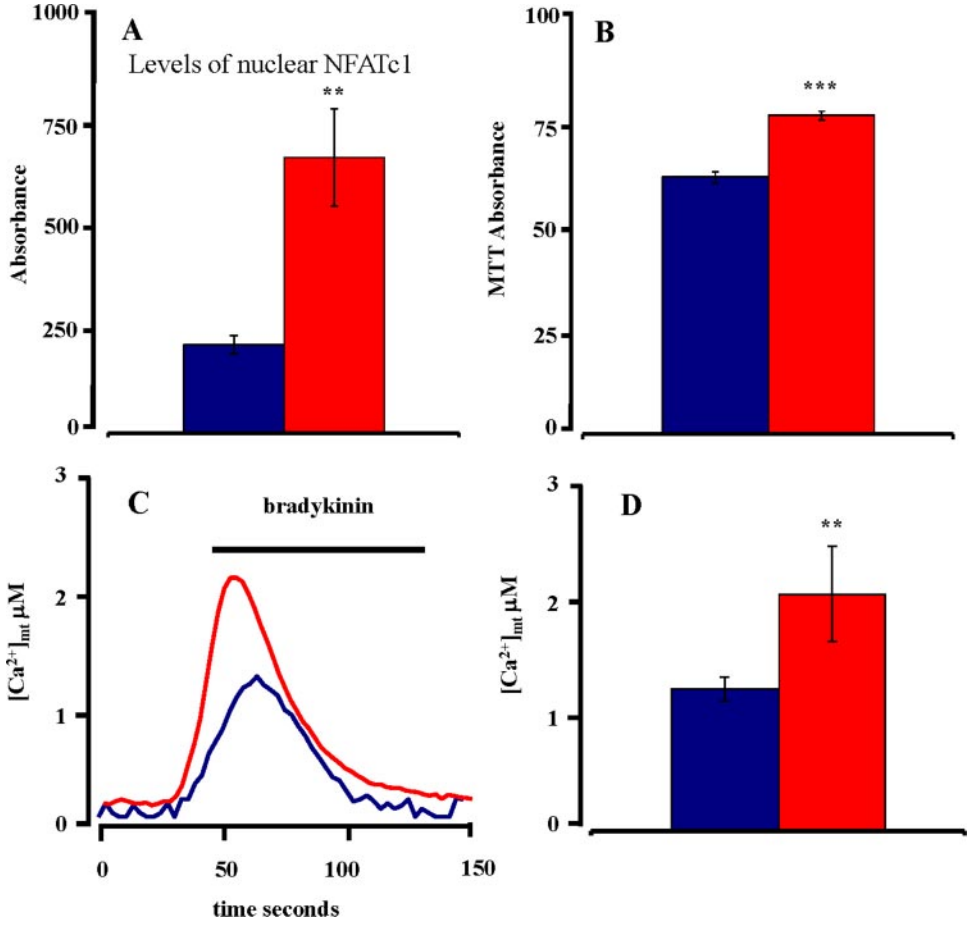

FIGURE 8. **P2X$_7$ transfection increases NFATc1 activation, proliferation and $[Ca^{2+}]_{mt}$ in NIH3T3 cells.** Mock transfected NIH3T3 cells blue bars, P2X$_7$-transfected NIH3T3 cells red bars. *A*, levels of nuclear NFATc1. The cells were transfected with P2X$_7$ or empty vector, 48 h after they were plated at a concentration of 10^6/dish in serum-free DMEM, incubated for 16 h, and assayed for NFATc1 translocation as described under "Experimental Procedures." *B*, proliferation was assayed with the 3-(4,5-dimethylthiazol-2-yl)-2,5-diphenyltetrazolium bromide (*MTT*) test as described under "Experimental Procedures." *C*, measurement of $[Ca^{2+}]_{mt}$. NIH3T3 cells were incubated in 1 mM Ca^{2+} supplemented standard saline (see "Experimental Procedures") and challenged with 1 μM bradykinin. *D*, summary data of repeated independent measurements ($n = 9$) of bradykinin-stimulated $[Ca^{2+}]_{mt}$ increases. **, $p < 0.01$; ***, $p < 0.001$.

sion reduces ER to mitochondria Ca^{2+} transfer. However, we were consistently unable to detect a reduction of ceramide-stimulated Ca^{2+} transfer from the ER to the mitochondria (data not shown); thus the site protection should be elsewhere. On the other hand, our findings suggest that the increased ER Ca^{2+} content primes P2X$_7$-expressing cells for resistance to apoptosis.

Our data point to a more substantial involvement of the NFAT pathway. NFAT is central for translating survival and growth signals mediated by increases in $[Ca^{2+}]_i$ (34, 48). We found that in HEK293-P2X$_7$ cells the level of NFATc1 nuclear translocation was at least twice as high as in control cells. This was not a mere correlation because NFATc1 blockade with the specific inhibitor peptide VIVIT or with cyclosporin fully abolished the growth advantage of HEK293-P2X$_7$ cells. Furthermore, VIVIT fully abolished the protective effect stemming from P2X$_7$R expression. This is consistent with previous data showing that pharmacological stimulation of the P2X$_7$R causes NFAT activation (49). VIVIT also slightly reduced survival of HEK293-mock cells, but this is not surprising because NFATc1 is basally activated also in the absence of the P2X$_7$R. Thus, it is possible that tonic activity of the P2X$_7$R, even in the absence of exogenous ATP, might drive increased nuclear localization of NFAT. This possibility is strongly suggested by the inhibitory effect of oATP or apyrase treatment on NFATc1 translocation. NFATc1 is increasingly recognized as a major transducer of growth or survival signals in normal or transformed cells; thus our data bring additional support to this role.

Our results dramatically underscore the opposite effects on cell physiology that basal *versus* stimulated activation of the very same receptor might have. Strong pharmacological stimulation of the P2X$_7$R with exogenous ATP or benzoyl ATP causes a cell catastrophe characterized by collapse of plasma membrane selectivity barrier, fragmentation of mitochondrial network, nuclear condensation, and cell death, to the point that the P2X$_7$R is often taken as a paradigm for cytotoxic receptors. On the contrary, basal activation has a profound trophic effect. Available data from this and previous works concordantly support the presence of basal channel activity of P2X$_7$R, even in the absence of added ATP: (*a*) removal of extracellular Ca^{2+} normalizes $[Ca^{2+}]_{mt}$; (*b*) treatment with oATP normalizes $[Ca^{2+}]_{er}$, $[Ca^{2+}]_{mt}$, and proliferation rate; and (*c*) treatment with apyrase or oATP normalizes $[Ca^{2+}]_{mt}$ and proliferation rate. This body of evidence strongly suggests that under physiological resting conditions the P2X$_7$R undergoes a tonic level of basal activation that allows a controlled influx of Ca^{2+}, which supports cell metabolism and cell growth avoiding the deleterious effect of unchecked Ca^{2+} entry because of pharmacological activation of the receptor. In this scenario, a crucial and still unsolved issue is how a low affinity ATP receptor, such as P2X$_7$R, is activated in conditions in which the extracellular ATP concentration should be exceedingly low. A few hypothesis can be put forward: local ATP release into protected sites close to the P2X$_7$R or the presence of additional factors that positively modulate P2X$_7$R activity. However, it is clear that additional experiments are needed to clarify this issue. In conclusion, we have provided evidence showing that basal activation of the P2X$_7$R has an anti-apoptotic effect and have identified NFATc1 as one of the pathways involved.

Acknowledgment—We are grateful to Dr. Cinzia Pizzirani for critically reading the manuscript.

REFERENCES

1. Di Virgilio, F., Chiozzi, P., Ferrari, D., Falzoni, S., Sanz, J. M., Morelli, A., Torboli, M., Bolognesi, G., and Baricordi, O. R. (2001) *Blood* **97,** 587–600
2. MacKenzie, A., Wilson, H. L., Kiss-Toth, E., Dower, S. K., North, R. A., and Surprenant, A. (2001) *Immunity.* **15,** 825–835
3. Morelli, A., Chiozzi, P., Chiesa, A., Ferrari, D., Sanz, J. M., Falzoni, S., Pinton, P., Rizzuto, R., Olson, M. F., and Di Virgilio, F. (2003) *Mol. Biol. Cell* **14,** 2655–2664
4. Pizzirani, C., Ferrari, D., Chiozzi, P., Adinolfi, E., Sandona, D., Savaglio, E., and Di, V. F. (2007) *Blood* **109,** 3856–3864
5. Chiozzi, P., Sanz, J. M., Ferrari, D., Falzoni, S., Aleotti, A., Buell, G. N., Collo, G., and Di Virgilio, F. (1997) *J. Cell Biol.* **138,** 697–706
6. Baricordi, O. R., Melchiorri, L., Adinolfi, E., Falzoni, S., Chiozzi, P., Buell, G., and Di Virgilio, F. (1999) *J. Biol. Chem.* **274,** 33206–33208
7. Di Virgilio, F., Chiozzi, P., Falzoni, S., Ferrari, D., Sanz, J. M., Venketaraman, V., and Baricordi, O. R. (1998) *Cell Death. Differ.* **5,** 191–199
8. Mackenzie, A. B., Young, M. T., Adinolfi, E., and Surprenant, A. (2005) *J. Biol. Chem.* **280,** 33968–33976
9. Gartland, A., Buckley, K. A., Bowler, W. B., and Gallagher, J. A. (2003) *Calcif. Tissue Int.* **73,** 361–369
10. Surprenant, A., Rassendren, F., Kawashima, E., North, R. A., and Buell, G. (1996) *Science* **272,** 735–738
11. Klapperstuck, M., Buttner, C., Schmalzing, G., and Markwardt, F. (2001) *J. Physiol.* **534,** 25–35
12. Steinberg, T. H., and Silverstein, S. C. (1987) *J. Biol. Chem.* **262,** 3118–3122
13. Di Virgilio, F. (1995) *Immunol. Today* **16,** 524–528
14. Virginio, C., MacKenzie, A., North, R. A., and Surprenant, A. (1999) *J. Physiol.* **519,** 335–346
15. Adinolfi, E., Callegari, M. G., Ferrari, D., Bolognesi, C., Minelli, M., Wieckowski, M. R., Pinton, P., Rizzuto, R., and Di Virgilio, F. (2005) *Mol. Biol. Cell* **16,** 3260–3272
16. Bonnet, S., Archer, S. L., lalunis-Turner, J., Haromy, A., Beaulieu, C., Thompson, R., Lee, C. T., Lopaschuk, G. D., Puttagunta, L., Bonnet, S., Harry, G., Hashimoto, K., Porter, C. J., Andrade, M. A., Thebaud, B., and Michelakis, E. D. (2007) *Cancer Cell* **11,** 37–51
17. Adinolfi, E., Melchiorri, L., Falzoni, S., Chiozzi, P., Morelli, A., Tieghi, A., Cuneo, A., Castoldi, G., Di Virgilio, F., and Baricordi, O. R. (2002) *Blood* **99,** 706–708
18. Slater, M., Danieletto, S., Gidley-Baird, A., Teh, L. C., and Barden, J. A. (2004) *Histopathology* **44,** 206–215
19. Slater, M., Danieletto, S., Pooley, M., Cheng, T. L., Gidley-Baird, A., and Barden, J. A. (2004) *Breast Cancer Res. Treat.* **83,** 1–10
20. Slater, M., and Barden, J. A. (2005) *Histopathology* **47,** 170–178
21. Greig, A. V., Linge, C., Healy, V., Lim, P., Clayton, E., Rustin, M. H., McGrouther, D. A., and Burnstock, G. (2003) *J. Investig. Dermatol.* **121,** 315–327
22. Raffaghello, L., Chiozzi, P., Falzoni, S., Di Virgilio, F., and Pistoia, V. (2006) *Cancer Res.* **66,** 907–914
23. Kunzli, B. M., Berberat, P. O., Giese, T., Csizmadia, E., Kaczmarek, E., Baker, C., Halaceli, I., Buchler, M. W., Friess, H., and Robson, S. C. (2007) *Am. J. Physiol.* **292,** G223–G230
24. Solini, A., Cuccato, S., Ferrari, D., Santini, E., Gulinelli, S., Callegari, M. G., Dardano, A., Faviana, P., Madec, S., Di, V. F., and Monzani, F. (2008) *Endocrinology* **149,** 389–396
25. Hillman, K. A., Burnstock, G., and Unwin, R. J. (2005) *Nephron Exp. Nephrol.* **101,** e24–e30
26. Rizzuto, R., and Pozzan, T. (2006) *Physiol. Rev.* **86,** 369–408
27. Rizzuto, R., Duchen, M. R., and Pozzan, T. (2004) *Sci. STKE.* 2004, re1
28. Choe, C. U., and Ehrlich, B. E. (2006) *Sci. STKE.* 2006, re15
29. Macian, F. (2005) *Nat. Rev. Immunol* **5,** 472–484
30. Martinez-Martinez, S., and Redondo, J. M. (2004) *Curr. Med. Chem.* **11,** 997–1007
31. Dumont, F. J. (2000) *Curr. Med. Chem.* **7,** 731–748
32. Lee, M., and Park, J. (2006) *Mol. Cells* **22,** 1–7
33. Viola, J. P., Carvalho, L. D., Fonseca, B. P., and Teixeira, L. K. (2005) *Braz. J. Med. Biol. Res.* **38,** 335–344
34. Buchholz, M., and Ellenrieder, V. (2007) *Cell Cycle* **6,** 16–19
35. Zayzafoon, M. (2006) *J. Cell. Biochem.* **97,** 56–70
36. Duque, J., Fresno, M., and Iniguez, M. A. (2005) *J. Biol. Chem.* **280,** 8686–8693
37. Yiu, G. K., and Toker, A. (2006) *J. Biol. Chem.* **281,** 12210–12217
38. Pinton, P., Rimessi, A., Romagnoli, A., Prandini, A., and Rizzuto, R. (2007) *Methods Cell Biol.* **80,** 297–325
39. Brini, M., Marsault, R., Bastianutto, C., Alvarez, J., Pozzan, T., and Rizzuto, R. (1995) *J. Biol. Chem.* **270,** 9896–9903
40. Barrero, M. J., Montero, M., and Alvarez, J. (1997) *J. Biol. Chem.* **272,** 27694–27699
41. Murgia, M., Hanau, S., Pizzo, P., Rippa, M., and Di Virgilio, F. (1993) *J. Biol. Chem.* **268,** 8199–8203
42. Chiozzi, P., Murgia, M., Falzoni, S., Ferrari, D., and Di Virgilio, F. (1996) *Biochem. Biophys. Res. Commun.* **218,** 176–181
43. Fulgenzi, A., Ticozzi, P., Gabel, C. A., Dell'Antonio, G., Quattrini, A., Franzone, J. S., and Ferrero, M. E. (2008) *Int. J. Immunopathol. Pharmacol.* **21,** 61–71
44. Pinton, P., Ferrari, D., Magalhaes, P., Schulze-Osthoff, K., Di Virgilio, F., Pozzan, T., and Rizzuto, R. (2000) *J. Cell Biol.* **148,** 857–862
45. Pinton, P., Ferrari, D., Rapizzi, E., Di Virgilio, F. D., Pozzan, T., and Rizzuto, R. (2001) *EMBO J.* **20,** 2690–2701
46. Scorrano, L., Oakes, S. A., Opferman, J. T., Cheng, E. H., Sorcinelli, M. D., Pozzan, T., and Korsmeyer, S. J. (2003) *Science* **300,** 135–139
47. Szabadkai, G., Simoni, A. M., Chami, M., Wieckowski, M. R., Youle, R. J., and Rizzuto, R. (2004) *Mol. Cell* **16,** 59–68
48. Gwack, Y., Feske, S., Srikanth, S., Hogan, P. G., and Rao, A. (2007) *Cell Calcium* **42,** 145–156
49. Ferrari, D., Stroh, C., and Schulze-Osthoff, K. (1999) *J. Biol. Chem.* **274,** 13205–13210